Chain of Circles for Matching and Recognition of Planar Shapes

Jae-Moon Chung and Noboru Ohnishi *
Bio-Mimetic Control Research Center
The Institute of Physical and Chemical Research (RIKEN)
2271-130 Anagahora, Shimoshidami, Moriyama-ku,
Nagoya, 463 Japan
E-mail: *chung@nagoya.riken.go.jp*

Abstract

Based on a resulting medial axis configuration of planar shapes, a new shape descriptor called the *chain of circles* (CoCs) is defined herein. The CoCs representation is directly extracted along the boundary contour of silhouette images, and can be controlled in a hierarchical manner which appeals to intuition. The coarse-to-fine hierarchy makes matching of shapes possible with less computational complexity and greater robustness to noise, spatial quantization and local deformation of shapes. The dissimilarity vector calculated in the matching, which is executed via the dynamic programming technique, may be used to facilitate the searching process in the digital library. The capability of the proposed method is shown by matching several complex shapes such as map images.

1 Introduction

Compared to the curvature-based shape descriptions [Mokhtarian and Mack worth, 1986; He and Kundu, 1991; Sederberg *et* a/., 1993; Siddiqi and Kimia, 1995], the axis-based methods [Blum, 1967; Blum and Nagel, 1978; Brady and Asada, 1984; Rosenfeld, 1986; Leyton, 1988; Saint-Marc *ei* al., 1993; Rom and Medioni, 1993; Zhu and Yuille, 1995; Ogniewicz and Kubler, 1995] are known to be capable of describing shapes in terms of the region surrounded by the boundary, as well as the boundary itself, simultaneously. Although this is not dealt with in this paper, we intuitively know that shapes with holes, as shown in Figure 1(a), also can be represented directly by the axis-based description without using any other intermediate representation.

Several axis-based descriptions [Blum and Nagel, 1978][Zhu and Yuille, 1995] require the analysis of axis connections to find branch points where shapes are partitioned into their parts. However, it is difficult to find stable branch points, as discussed in [Zhu and Yuille, 1995], in which they used a top-down approach using shape models to solve the problem, which can deal with only the formal shapes, as shown in Figure 1(b). Blum's medial axis transformation (MAT) [Blum, 1967] and its effective calculation [Lee, 1982] has conventionally been used to calculate the axis. However, the use of MAT has been criticized because the axis obtained is very sensitive even to a slight deformation of shapes, as shown in Figure 1(c). Although several ideas [Blum and Nagel, 1978][Ogniewicz and Kiibler, 1995] have been proposed to solve this problem, a more systematic approach is required.

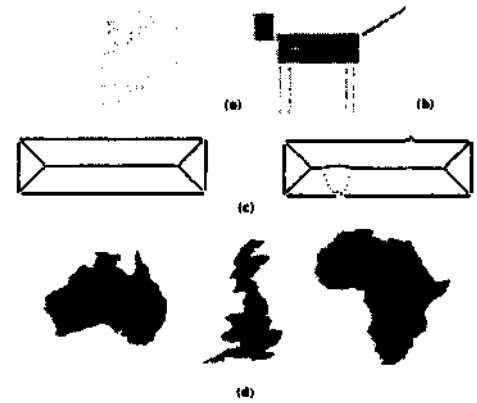

Figure 1: (a) A planar shape with a hole, (b) An example of formal shapes, (c) The rectangle can be described using the axis obtained by applying medial axis transformation to its boundary contour (left), but the description is greatly affected by even a slight deformation of the contour (right), (d) Examples of nonformal shapes. These are difficult to describe using verbal representation and to decompose into parts.

In this paper, we present a new planar shape description called the *chain of circles* (CoCs). As an axis (or region)-based representation, the CoCs is rich and invariant to rotation and translation of shapes. The CoCs also has hierarchical description capability, i.e, the capability to represent shapes at various levels of detail on demand. Using this capability, it is shown how we can get robust representation against noise and local deformation of shapes. Examples of shape matching and recognition using the CoCs are presented for fairly complex shapes such as those shown in Figure 1(d).

2 Chain of Circles

2.1 Medial Axis Transformation

*He is also with Dept. of Information Eng., School of Eng.. Nagoya Univ., Japan

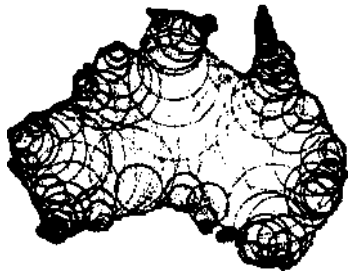

Figure 2: A collection of the maximal disks (MDs) obtained for the inner part of a map of Australia. A maximal disk has its center at a point on the medial axis of the boundary curve.

The idea of MAT was developed by Blum [Blum, 1967] to extract the medial (or symmetric) axis of planar shapes. From the physics of *grass fire*[1] it can be said that the medial axis is uniquely determined for a planar shape.

The medial axis generated by applying MAT to a boundary curve can also be considered as the locus of the center of the maximal disk (MD), as shown in Figure 2. MD is a circle which does not cross the boundary curve and touches at least two points on the curve. Several algorithms have been proposed for effective computation of MAT of a curve approximated by a polygon [Lee, 1982]. The vertexes of the polygon are sampling points on the curve.

2.2 Chain of Circles (CoCs)

As shown in Figure 3(a), in shapes represented by a collection of MDs, a MD generally has two points x_1 and x_2 which contact the boundary contour of the shapes. The two points are mutually corresponding. The correspondence arises from the fact that the two contact points share a common MD. The CoCs is defined by $r(x)$ and $\phi(x)$ along the arc length x of a boundary contour curve. (See Appendices A and B for proof of the validity of the CoCs as a shape representation).

At each point, for example x_1 the MD is described by $r(x_1)$ the radius of the MD and $\phi(x_1)$ the angle from x_1 to the corresponding point X_2 around the center of the MD in the clockwise direction. The point x_2 is described in the same manner. The range of $\phi(x)$ is between 0 and 2π $[rad]$.

Although the CoCs can be extracted for both the internal area and the exterior of the boundary contour of shapes, we here use only the internal area, as shown in Figures 3(b) and (c). Depending on the local geometry of shapes, there is a MD that has more than two contact points. For the uniqueness of description in this case, we use a $\phi(x)$ value closest to π.

[1] In the case that we fire the boundary line of a shape written on grass simultaneously, the line of extinction is uniquely determined depending on the shape.

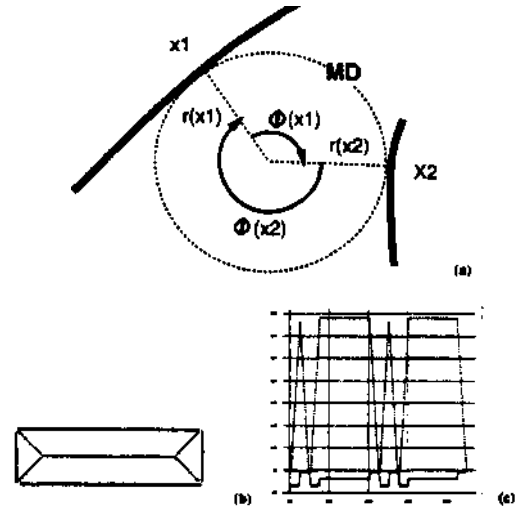

Figure 3: Definition of chain of circles, represented by (a) $r(x)$ and $\phi(x)$ along contour arc length x. (b) A rectangle and its axis, (c) Extracted CoCs representation for one rotation of (b) starting from the upper left corner and moving in a clockwise direction. The dotted and solid lines correspond to $r(x)$ and $\phi(x)$, respectively.

2.3 Control of CoCs: Robust Description

Prior to describing the control of CoCs, we redefine v(x) and $r_n(x)$ as

$$r_n(x) = \frac{r(x)}{r_{max}} 100, \quad (0 \le r_n(x) \le 100) \tag{1}$$

$$\vartheta(x) = \frac{\phi(x)}{2} \quad if\ 0 \le \phi(x) \le \pi, \tag{2}$$

$$\vartheta(x) = \frac{2\pi - \phi(x)}{2} \quad otherwise,$$

$$(0 \le \vartheta(x) \le 90^o),$$

where $r_n(x)$ denotes the normalized percentage of $r(x)$ to r_{max} which is the radius of the largest MD in the CoCs representation of a shape, and is set to 100.

As observed in [Blum and Nagel, 1978][Ogniewicz and Kübler, 1995], we consider that MDs with small values of $r_n(x)$ and $\vartheta(x)$ in a CoCs representation localize only noise or very small corner features. Following this observation, here the criterion for controlling the CoCs representation is set as,

$$[r_n(x) + r_c][\vartheta(x) + \vartheta_c] = \Gamma, \tag{3}$$

$$(0 \le \Gamma \le 9000),$$

where r_c and ϑ_c are bias values corresponding to $r_n(x)$ and $\vartheta(x)$, respectively.

Figure 4 shows the criterion for controlling the CoCs representation based on equation (3). Among whole MDs in the CoCs representation of a shape, only MDs corresponding to the right side of a line are used in the description of a shape. Using a set of parameter values of equation (3), the CoCs representation in Figures 3(b) and (c) is reconstructed as shown in Figure 5.

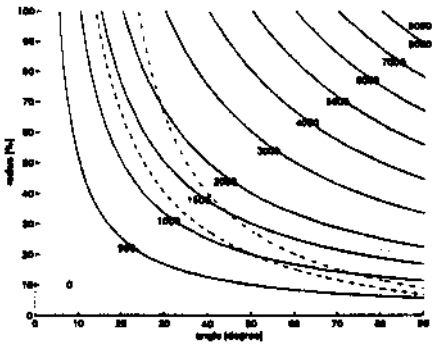

Figure 4: Control of CoCs. Each numeral on solid lines indicate T values when both r_c and v_c are 0. The dotted line is for (r=1500, r_r=0, v_c=-10), the dashed line (1500,10,0) and the dot-dash line (1500,10,-10).

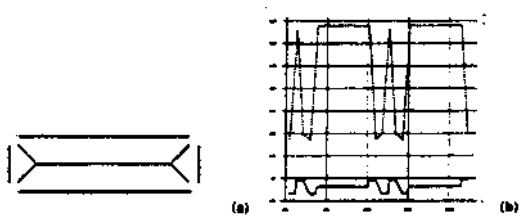

Figure 5: Controlled CoCs representations with r=1500, $r_c=0$ and $\dot{v}_c=0$. (a) The thick points on the boundary contour line display contour points used in each representation, and thin points show unused points, (b) The lines show interpolated results for unused contour points using the neighboring used contour points.

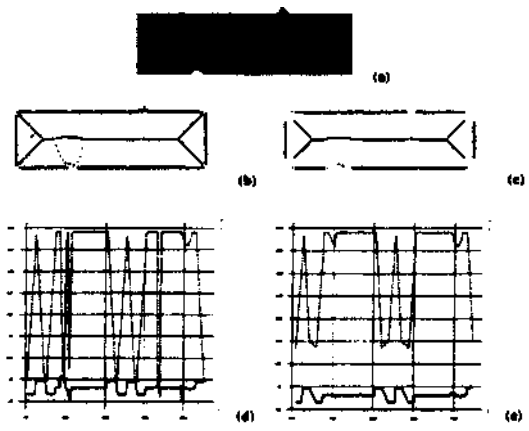

Figure 6: (a) A notched image of the rectangle. (b)(d) Uncontrolled and (c)(e) controlled CoCs representations.

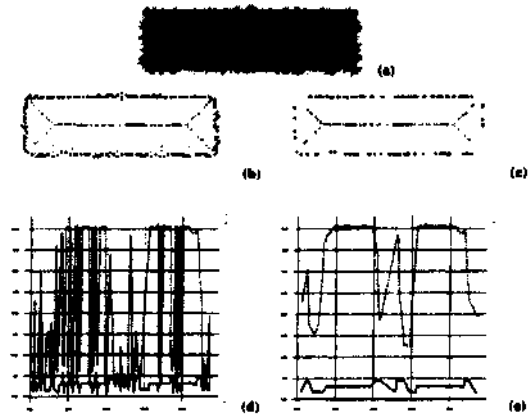

Figure 7: (a) A noisy image of the rectangle. (b)(d) Uncontrolled and (c)(e) controlled CoCs representations.

Figures 6 and 7 show the robustness of shape description obtained from the control of the CoCs representation. The parameter values used are the same as those used in Figure 5. Note that Figures 6(e) and 7(e) become similar to Figure 5(b) due to the control, even though their uncontrolled original was corrupted.

3 Hierarchical Approximation of Nonformal Shapes

Figure 8 shows how nonformal shapes are hierarchically approximated based on CoCs representation. The values of parameters $\dot{r}_c$ and $\dot{\vartheta}_c$ in equation (3) are selected to be 10 and —10, respectively. The hierarchy of the description is obtained by controlling the value of T. Figure 9 shows the corresponding CoCs representation.

4 Matching and Recognition

4.1 Matching Using DP

The dynamic programming (DP) technique is used to match a pair of CoCs representations. We can expect computational efficiency because matching is possible based on the ordering constraint, as used in [Sakoe and Chiba, 1978; Geiger *et al,* 1995].

If there are / points in one and J points in the other of a pair of CoCs which must be matched, and / is greater than /, a match sequence of length A" is a set of point matches P, as

$$P = \{(i(k), j(k)) | 1 \le i(k) \le I, \quad 1 \le j(k) \le 2J, 1 \le k \le K \le I + J\}, \tag{4}$$

where twice the number of J points must be made for a match which does not depend on starting points of the two CoCs representations in the matching process. The score 5 for the match sequence P is defined as the sum of the individual similarity scores s as

$$S = \sum_{k=1}^{K} s(i(k), j(k)). \tag{5}$$

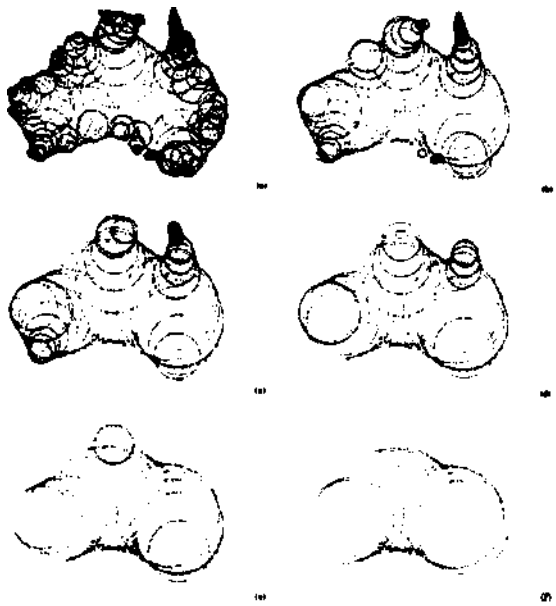

Figure 8: The hierarchical approximation of the map of Australia, each of which is displayed as the collection of MDs used. The values of *T* and the numbers of contour points are (a) 0, 204 points (b) 1000, 98 (c) 1500, 66 (d) 2000, 46 (e) 3000, 32 and (f) 4000, 23, respectively.

The problem in matching is to find the match sequence with the highest score, and the computational complexity corresponds to the number of steps, $O(I^2(2J)^2)$ [Ota and Kanade, 1985]. Here the individual similarity score is defined as

$$s(i,j) = s_{max} - [w_r\ |r_n(i) - r_n(j)| + w_\phi\ |\phi(i) - \phi(j)| + w_x\ |\delta x(i) - \delta x(j)|],$$

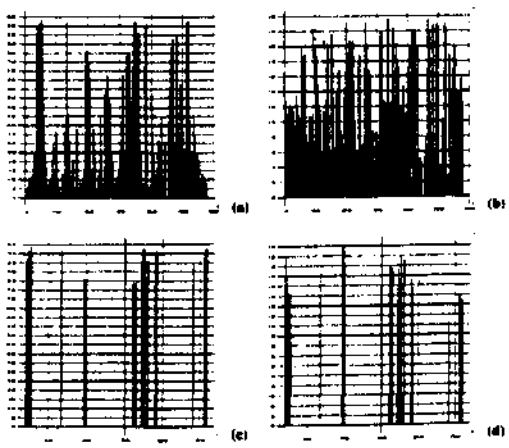

Figure 9: The CoCs representations for the map of Australia. (a) $r(x)$, (b) $\phi(x)$ for Figure 8(a), and (c) $r(x)$, (d) $\phi(x)$ for Figure 8(f).

where s_{max} is a reference value, and w_ϕ, w_r and w_x are weighting factors for each difference for a point pair between two CoCs representations, and δx denotes the distance between a point and its previously matched point on each contour line.

4.2 Dissimilarity Vector for Recognition

For the matched pairs of shapes, the dissimilarity vector *D* is calculated by averaging each of the differences of r, ϕ and δx between the matched points as

$$\vec{D} = \frac{1}{K}\sum_{k=1}^{K}[|r_i(k) - r_j(k)|, \quad |\phi_i(k) - \phi_j(k)|, |\delta x_i(k) - \delta x_j(k)|], \tag{7}$$

where A denotes the number of matched points between two CoCs representations.

4.3 Computational Complexity

Figure 10 shows an example of computational complexity for self-matching of CoCs representations shown in Figure 8. From this, we can see that computational complexity in the matching process is greatly reduced by using the approximated shape representation of the CoCs. Compared to matching with no approximation (T=0), which takes about 1 *hour,* for example, matching with an approximation (T=3000) takes just 1 *s.*

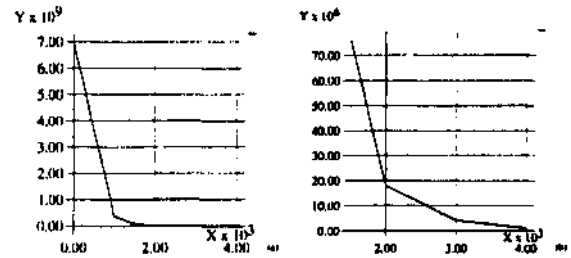

Figure 10: Computational complexity depending on the value of *T:* (a) global and (b) local displays. The horizontal and vertical axes are for the degree of shape approximation denoted by the values of T, and computational complexity in matching, respectively.

5 Experiments

In the experiment, r_n and ϕ on each point of two curves are normalized so that their maxima become 100. δx is also normalized so that the length of each of the two curves becomes 100. In the implementation of matching, the values of parameters in equation (6) were s_{max}=1000, w_r=3, w_ϕ= 3 and w_x=9. Figures 11 and 12 and Table 1 show shapes used in the experiment, matching results and dissimilarity values used for recognition, respectively.

6 Discussions

Figure 14 shows the robustness of the controlled CoCs to digitization of shapes. With much computational efficiency, matching using the approximated CoCs was successful not only for variously disturbed shapes, but for

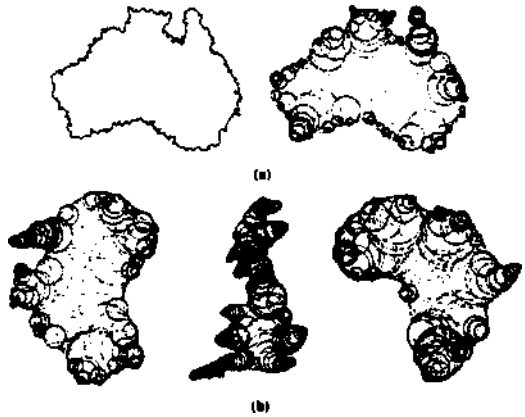

Figure 11: Shapes used in experiments, (a) A noisy image of the map of Australia and its display of collection of MDs. (b) Collections of MDs to the maps of rotated Australia, England and Africa, for T = 0. Rotated Australia is used to investigate the effect of spatial quantization arising from the shift of sampling points on the contour curve.

different shapes, as shown in Figure 12, in which the correctness may be improved, by some means, in the programming of the method. The matching of different shapes is necessary for searching shapes from a digital database.

Table 1 shows that the dissimilarity vector calculated via matching has different values depending on the resemblance between shapes. The values of self-matching *(Aus)* and matching with disturbed shapes *(n(A)* and *r(A))* are zero and relatively small, respectively. As expected, the Australia-England match *(Eng)* has much higher dissimilarity than the Australia-Africa match *(Afr)*.

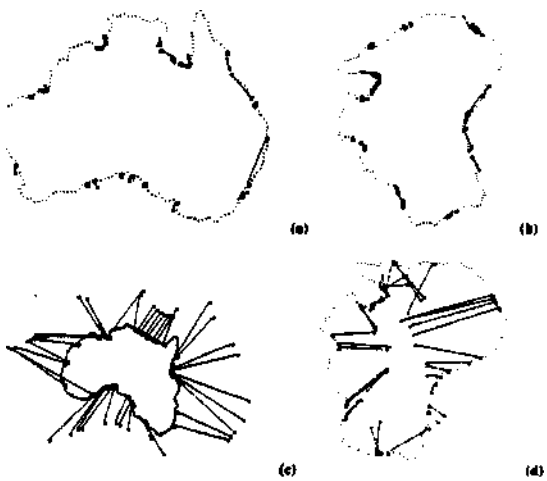

Figure 12: The results of matching of the map of Australia to (a) its noisy and (b) oriented images, and (c) the maps of Africa and (d) England. In each of the matches, squares show the contour points determined in matching among the points used in each CoCs representation (T = 2000). The lines connecting the squares show matched points between two contour lines.

Table 1: The dissimilarity vectors between the map of Australia (shown in Figure 8) and the shapes shown in Figure 11 when case of the values of T are 2000 and 3000. The columns of *Aus, n(A), r(A), Afr* and *Eng* are for self-matching of Australia, matching of Australia to noisy Australia, rotated Australia, Africa and England, respectively.

	Γ=2000	Γ=3000
Aus	(0,0,0)	(0,0,0)
n(A)	10.5(0.71,0.65,0.26)	12.9(0.77,0.56,0.28)
r(A)	9.8(0.33,0.74,0.57)	11.2(0.15,0.72,0.67)
Afr	16.1(0.71,0.67,0.12)	14.1(0.77,0.59,0.22)
Eng	40.0(0.95,0.22,0.21)	27.6(0.86,0.32,0.36)

Fundamentally, open curve matching is also possible based on the CoCs if the greatest MD in each curve is determined. Although the determination seems to be possible via iteration, we expect to obtain a more concrete approach by a theoretical analysis on the CoCs.

A Local Geometric Analysis

As shown in Figure 13, the local geometry of the shape represented by a collection of MDs is analyzed as follows. If *y(s)* denotes a vector from the origin of a coordinate system to the center of a MD, i.e., a vector on an arc length s of the axis, x a vector from the origin to a point on the edge of the MD, and r(s) the radius of the MD, the shape can be formulated as

$$G(\boldsymbol{x}, \boldsymbol{y}(s), s) = [\boldsymbol{x} - \boldsymbol{y}(s)] \cdot [\boldsymbol{x} - \boldsymbol{y}(s)] - r^2(s) = 0. \quad (8)$$

Because the envelope of the collection of these MDs arises from the intersection of two adjacent MDs, it can be calculated from

$$\frac{\partial G(\mathbf{x}, \mathbf{y}(s), s)}{\partial s} = 0. \quad (9)$$

From equation (9), we can deduce

$$\dot{\boldsymbol{y}}(s) \cdot [\boldsymbol{x} - \boldsymbol{y}(s)] = -r(s)\dot{r}(s), \quad (10)$$

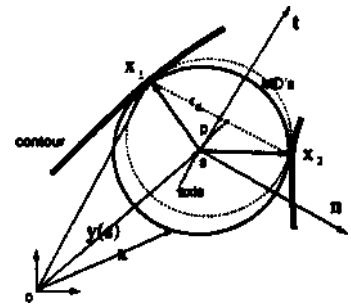

Figure 13: Local geometry of MDs.

where *y(s)* and *r(s)* denote the derivatives of *y(s)* and r(s) with respect to s, respectively, and y(s) is in the tangential direction of the axis on *s*.

Let $\vec{t}$ be the unit tangent vector to the axis curve and formed with the unit normal vector $\vec{n}$. An orthonormal frame $\vec{t}$-$\vec{n}$ is a moving frame and a function of arc length s along the axis curve, as shown in Figure 13. At every intersection point between MDs, a vector *x-y(s)* makes an angle with an unit tangent vector $\vec{t}$. From equation (9), the value of the angle $\theta(s)$ is

$$\theta(s) = \arccos[-\dot{r}(s)]. \qquad (11)$$

As shown in Figure 13, cross-sectional points of MDs are rewritten for the $\vec{t}(s)$-$\vec{n}(s)$ frame as

$$x_{1,2}(s) = y(s) \pm r_d(s)\vec{n} + p(s)\vec{t}, \qquad (12)$$

where $r_d(s)=r(s)\sin\theta$ and $p(s) = r(s)\cos\theta$.

The following differential equations are satisfied by the $\vec{t}(s)$-$\vec{n}(s)$ frame:

$$\frac{\partial y(s)}{\partial s} = \vec{t}, \quad \frac{\partial \vec{t}}{\partial s} = \kappa(s)\vec{n}, \quad \frac{\partial \vec{n}}{\partial s} = -\kappa(s)\vec{t}, \qquad (13)$$

where $\kappa(s)$ is the curvature of the axis curve at s.

The $\vec{t}(s)$-$\vec{n}(s)$ frame is moving and is a function of arc length s. If we use r, $\dot{r}$, $\ddot{r}$ and κ instead of $r(s)$, $\dot{r}(s)$, $\ddot{r}(s)$ and $\kappa(s)$, respectively, the relative variation of contour points can be derived from equations (12) and (13) as

$$\dot{x}_{1,2}(s) = [1 \mp r(1-\dot{r}^2)^{1/2}\kappa - (\dot{r}^2 + r\ddot{r})]\vec{t} + \dot{r}[r\kappa \pm (1-\dot{r}^2)^{1/2} \pm r\ddot{r}(1-\dot{r}^2)^{-1/2}]\vec{n}. \qquad (14)$$

When $\dot{r}^2(s)$ and $\ddot{r}(s)$ are much smaller than 1 [2], equation (14) becomes

$$\dot{x}_{1,2}(s) = [1 \mp r\kappa]\vec{t} \pm \dot{r}[1 \pm r\kappa]\vec{n}. \qquad (15)$$

Equation (15) indicates that a planar shape can be represented by radius parameters $r(s)$ and $\dot{r}(s)$ of MDs, and axis parameters $\kappa(s)$, $\vec{t}(s)$ and $\vec{n}(s)$ along the arc length of axis s. In addition, equation (11) indicates that $\dot{r}(s)$ is directly related to $\theta(s)$. The effect of axis parameters in CoCs representation will be briefly discussed in **B**.

B Global Geometric Property

Compared to Figure 5(b), Figure 14(d) shows that the bending of the axis is reflected in the CoCs representation. There is an apparent difference in the lengths of the upper and lower edges between the two figures.

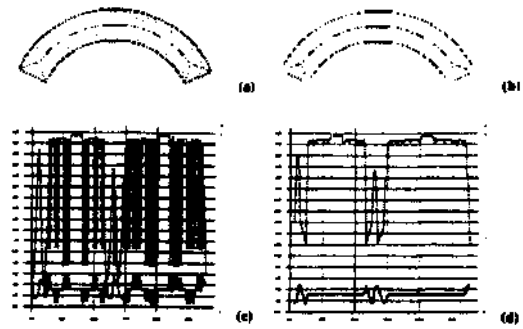

Figure 14: Bending of a rectangle. (a)(c) The uncontrolled and (b)(d) controlled shapes and CoCs representations (T = 1500).

References

[Mokhtarian and Mackworth, 1986] F. Mokhtarian and A. Mack worth. Scale-based description and recognition of planar curves and two-dimensional shapes. *IEEE Trans. Pattern Anal. Mach. IntclL,* 8(I):34-43, 1986.

[He and Kundu, 1991] Y. He and A. Kundu. 2-D shape classification using hidden markov model. *IEEE Tr. PAMI,* 13(11):1172-1184, 1991.

[Sederberg *et* al., 1993] T. W. Sederberg, P. Gao, G. Wang, and H. Mu. 2-D shape blending: an intrinsic solution to the vertex path problem. *Computer Graphics,* pages 15-18, 1993.

[Siddiqi and Kimia, 1995] K. Siddiqi and B. B. Kimia. Parts of visual form: computational aspects. *IEEE Tr. PAMI,* 17(3):239-251, 1995.

[Blum, 1967] H. Blum. A transformation for extracting new descriptors of shape, In W. Wathen-Dunn, editor, *Models for perception of speech and visual form,* MIT Press, 1967.

[Blum and Nagel, 1978] H. Blum and R. N. Nagel. Shape description using weighted symmetric axis features. *Pattern Recog.,* 10:167-180, 1978.

[Brady and Asada, 1984] M. Brady and H. Asada. Smoothed local symmetries and their implementation. *Int. J. Robotics Research,* 3(3):36-60, 1984.

[Rosenfeld, 1986] A. Rosenfeld. Axial representations of shape. *Comput. Vision Gr. Image Proc.,* 33:156-173, 1986.

[Ley ton, 1988] M. Leyton. A process-grammer for shape. *Artificial Intelligence,* 34:213-247, 1988.

[Saint-Marc *et al.,* 1993] P. Saint-Marc, H. Rom, and G. Medioni. B-spline contour representation and symmetry detection. *IEEE Tr. PAMI,* 15(11):1191-1197, 1993.

[Rom and Medioni, 1993] H. Rom and G. Medioni. Hierarchical decomposition and axial shape description. *IEEE Tr. PAMI,* 15(10):973-981, 1993.

[Zhu and Yuille, 1995] S. C. Zhu and A. L. Yuille. FORMS: a flexible Object recognition and modeling system. *Proc. ICCV'95,* pages 465-472, 1995.

[Ogniewicz and Kubler, 1995] R. L. Ogniewicz and O. Kubler, Hierarchic voronoi skeletons. *Pattern Recog.,* 28(3):343-359, 1995.

[Lee, 1982] D. T. Lee. Medial axis transformation of a planar shape. *IEEE Tr. PAMI* 4(4):363-369, 1982.

[Sakoe and Chiba, 1978] H. Sakoe and S. Chiba. Dynamic programming algorithm optimization for spoken word recognition. *IEEE Tr. Acous. Speech Sig. Proc.,* 26(1):43-49, 1978.

[Geiger *et al,* 1995] D. Geiger, A. Gupta, and J. Vlontzos. Dynamic programming for detecting, tracking, and matching deformable contours. *IEEE Tr. PAMI,* 17(3):294-302, 1995.

[Ota and Kanade, 1985] Y. Ota and T. Kanade. Stereo by intra- and inter-scan line search using dynamic programming. *IEEE Tr. PAMI* 7(2):139-154,1985.

[2] This condition corresponds to a controlled representation of shapes with a large value of *V*.